MADRID
inter.noise 2019
June 16 - 19
NOISE CONTROL FOR A BETTER ENVIRONMENT

Aeroacoustic Analysis of Coaxial Rotor with Rotor-Fuselage Interaction

Kim, Jonghui[1]
Ko, Jeongwoo[2]
Lee, Soogab[3]

Department of Mechanical and Aerospace Engineering, Seoul National University
Seoul, 151-744, Republic of Korea

ABSTRACT

This study investigates the aeroacoustic characteristics of a coaxial rotor with rotor-fuselage interaction. Compared to the conventional single rotor, the coaxial rotor can satisfy higher aerodynamic performances and recently it is proposed for Unmanned or Personal Aerial Vehicles due to its advantages and improved performance. It is required to predict accurately the aerodynamic and aeroacoustic performances with various operating configurations. In this study, a numerical analysis was conducted to identify the aerodynamic and aeroacoustic characteristics of the coaxial rotor with rotor-fuselage interaction based on free wake vortex lattice method and Ffowcs-Williams Hawkings equation. The fuselage surface is consisted of Source and doublet panels to enable considering interaction with the wake and the rotor. We observed that the thrust of the coaxial rotor with fuselage is lower than that of the isolated coaxial rotor in case of the level flight. We also observed that the thrust fluctuation of the coaxial rotor with fuselage is higher than that of the isolated coaxial rotor. Although the coaxial rotor has its own unsteadiness, the fuselage has quite intensified the pressure fluctuations of the blade surface affecting the unsteady loading noise. As a result, the aeroacoustic characteristics (such as the amplitudes and directivities) of the coaxial rotor with fuselage differs significantly from the isolated coaxial rotor.

Keywords: Aeroacoustics, Vortex Lattice Method, Rotor-Fuselage Interaction
I-INCE Classification of Subject Number: 13

---

[1] speedbobs@snu.ac.kr
[2] gowoo1314@snu.ac.kr
[3] solee@snu.ac.kr

1. INTRODUCTION

Since the invention of the rotorcraft, the necessity of rotary aircraft has been increased gradually in the military or civil industry. In recent years, its importance is further highlighted by the improvement of drones. Furthermore, Various types of compound rotorcraft like coaxial or ducted fan have been studied to overcome shortcomings of a conventional helicopter. The tail rotor to offset opposite moment of the fuselage is not necessary for the coaxial rotor sharing the same axis of rotation but turning in opposite directions. Rotorcrafts that need sufficient thrust within the limited design condition can be miniaturized with this advantage. Although, it needs to be consumed more computation costs and is hard to predict precisely aerodynamic performances to consider more complexities than the single rotor. The effort is required to understand the physical phenomena of the complex flow generated by the shed wake from the rotor. The major reasons are related to the aerodynamic interactions among the rotor, the wake and the fuselage consisting of the flow around the rotor. Though there have been sufficient studies on the rotor-fuselage interaction from the past, the research is needed on efficient analysis tool that can still maintain high accuracy and low computational cost. In addition, by predicting the aeroacoustic results of the coaxial rotor with rotor-fuselage interaction, it is possible to confirm the more realistic aeroacoustic characteristics.

Most previous studies have been focused on the prediction and understanding of aerodynamic characteristics. Representatively, Coleman's review paper presents the research trends about coaxial rotors with the broad investigation. The studies progressed by USA, Russia, U.K., and Japan until the late 20th century are extensively included.[1] The computational study on the aeroacoustic characteristics difference between the isolated coaxial rotor and the equivalent sing one is conducted by H. Kim based on VTM method. [2] The previous experimental research of aeroacoustic characteristics is studied by Mosher et al. In this investigation, it is described that a comparison of the sound generating trends of the coaxial rotor against the single rotor in several aviation conditions. [3] The precedent studies on the rotor-fuselage interaction effect of the single rotor have focused mainly on aerodynamic performance. Wilson et al conducted the experimental measurements on the interaction between the shed wake from the coaxial rotor and the fuselage. [4] Sheridan et al progressed experiments in the wind tunnel on the aerodynamic characteristics using a combination of various rotor and fuselage configurations. [5] Jang et al proposed an analysis of unsteady pressure fluctuation on the fuselage surface by using Poisson equation. It has the advantage to calculate the surface pressure of fuselage rather than the unsteady Bernoulli equation.[6] In order to reduced computational cost and simulate the complex wake flow efficiently, free wake vortex lattice method and FW-H acoustic analogy was used to analyze the aeroacoustic characteristics of the coaxial rotor with rotor-fuselage interaction.

2. Methodology

2.1 Aerodynamics

If the flow of an arbitrary blade excluding the boundary and wake region is assumed to be incompressible, inviscid and irrotational, the governing equation of the velocity potential < ϕ > can be represented by Laplace equation.

$$\nabla^2\phi = 0 \qquad \text{(Eq. 1)}$$

A general solution consisting of source and doublet panel distributed on boundary layer of the blade can be obtained by Green's reciprocity theorem. If the thin blade is applied, the effect of the source term is negligible. The doublet distribution on an approximated surface along the camber line replaces a vortex lattice whose strength is equivalent to that of the doublet. [7]

$$\left\{\int_{\text{blade}} \Gamma \frac{\partial}{\partial n}\left(\frac{1}{r}\right) dS - V_{\mathrm{B}} + V_{\text{wake}} + V_{fuselage}\right\} \cdot n = 0 \qquad \text{(Eq. 2)}$$

Where < Γ > is the vortex strength (circulation). The boundary condition for the singularity is applied by Dirichlet condition to be zero tangential velocity. Also, <V_{B}> is blade surface velocity by rotating, <V_{wake}> and <V_{fuselage}> are the induced velocities by the rotor wake and the fuselage, respectively. The velocity induced by the other vortex element is calculated by the parabolic Biot-Savart integral. [8] Vortex filaments is generated along the spanwise direction of the trailing edge and shed. At each time step, vorticities of trailed vortex lattices can be obtained from the vortex strength of the former one with Kutta condition and free wake elements are moved with the local velocity induced by the other blade, wake elements and the fuselage. Aerodynamic performances are described by using the unsteady Bernoulli equation. -Vorticity contour model is applied to the efficient calculation of wake filament- The Scully's vortex core model is applied to avoid the singularity at the vortex core. [9]

The fuselage is represented by source and doublet panel of constant strength based on the potential theory. It is the same as the blade, but, the fuselage cannot be assumed to a thin surface. Therefore, the source terms are considered to simulate the complex flow. In this unsteady flow, source terms are described as follows: [10]

$$\sigma = \left(V_{\mathrm{F}} - V_{\text{blade}} - V_{\text{wake}}\right) \qquad \text{(Eq. 3)}$$

Where <V_{F}> is the fuselage surface velocity, <V_{blade}> is the velocity induced by the blade excluding the wake. The doublet terms are calculated by using the Laplace equation the same as that of the blade. The surface pressure on the fuselage is calculated by the unsteady Bernoulli equation.

2.2 Aeroacoustics

The aeroacoustic computation is implemented by Ffowcs-Williams Hawkings (FW-H) acoustic analogy for the impermeable surface to analyze aeroacoustic characteristics considered with the rotor-fuselage interaction effect. [11] The tip Mach number of rotorcrafts is limited within the transonic region, therefore the nonlinear quadrupole noise term could be neglected. The sound source surface is set to the blade surface pressure distribution of the coaxial rotor. The equations of the impermeable FW-H are as follows in Equations 4 and 5. Each component is thickness and loading noise which are the discrete frequency noise of the rotor blade. The thickness noise is generated by the flow rate which is induced by the blade rotating motion, so it is related to the blade shape and the speed of rotation as Equation 4. The loading noise is generated by pressure and time derivative of pressure on the blade surface as Equation 5

$$4\pi p_T'(x,t) = \int_{f=0} \left[\frac{\rho_0 \dot{v}_n}{r(1-M_r)^2} + \frac{\rho_0 v_n \hat{r} \dot{M}_r}{r(1-M_r)^3}\right]_{ret} ds + \int_{f=0} \left[\frac{\rho_0 v_n c_0 (M_r - M^2)}{r^2(1-M_r)^3}\right]_{ret} ds \qquad \text{(Eq. 4)}$$

$$4\pi p_L'(x,t) = \frac{1}{c_0}\int_{f=0} \left[\frac{\dot{p}\cos\theta}{r(1-M_r)^2} + \frac{\hat{r}\dot{M}_r p\cos\theta}{r(1-M_r)^3}\right]_{ret} ds + \int_{f=0} \left[\frac{p(\cos\theta - M_i n_i)}{r^2(1-M_r)^2} + \frac{(M_r - M^2) p\cos\theta}{r^2(1-M_r)^3}\right]_{ret} ds$$

(Eq. 5)

3. Numerical Results

3.1 Verification

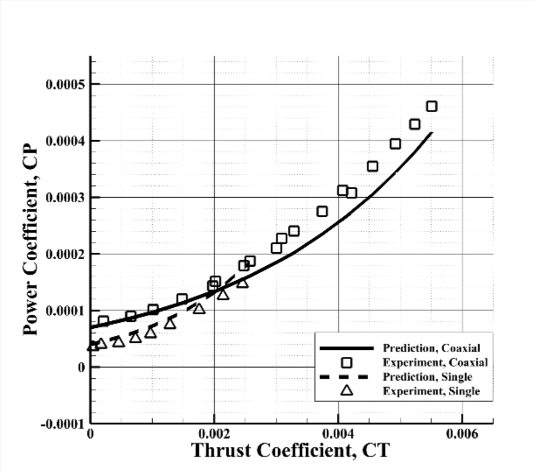

Figure 1 Comparison of power coefficient of coaxial rotor against a single rotor in hovering

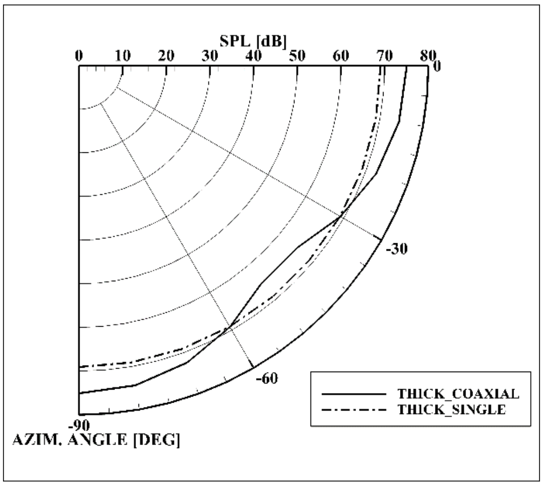

Figure 2 Comparison of the thickness noise level of coaxial rotor against a single rotor

Several tests are conducted to verify the reliability of the developed tool for the coaxial rotor in case of hovering. Figure 1 shows a comparison between the experimental measurements of the power coefficient versus the thrust coefficient and the data calculated by the prediction tool. While the computational data is slightly underpredicted within higher the thrust coefficient regions, the trend of others is captured well with the experimental ones. It can be seen that the power consumption at zero thrust of the coaxial rotor is twice than the single one, it means that the profile drag of the coaxial one is twice than the single one. Figure 2 shows a comparison of the in-plane directivities of the thick noise levels between the single rotor and the coaxial one. At 0 degree of the azimuth angle, it can be seen that the thickness noise level of the coaxial rotor is 6 dB higher than the result of the single one, because of the same sound pressure levels and phase angles between the upper and lower rotor. Conversely, it can be seen that the level of the coaxial one is 6 dB lower than the level of the single one at -45 degree of the azimuth angle. Therefore, the noise characteristics of the coaxial rotor are dominant by the phase difference between the upper and lower rotor. The described agreements well regarded between the performances of the coaxial rotor against the single one lend confidence in the ability of the prediction tool based on potential flow to provide simulation results considering the rotor-fuselage interaction with reliability.

3.2 Discrete Frequency Noise

The fuselage modeled by a rectangular source-doublet plate consisting of 3000 (30x100) grid cells. The reason why choose the only simple shape for fuselage is due to the fact that it is sufficient and suitable for this basic study to predict of aeroacoustic effects by rotor-fuselage interaction. In the next future work, it plans to be applied to cylindrical shape like ROBIN model used by NASA to simulate more practical results. [12] The coaxial rotor consists of a two-bladed teetering rotor. The blade has continuous six airfoil sections from NACA0031 to NACA0012 and a simple rectangular planform with no twist. The rotor radius is 12.5 ft and 8 degrees for the collective pitch angle. The inter rotor spacing is 2.33 ft, the fuselage is located at 1.5 ft below the lower rotor and the surface mesh of each blade consists of 300 structured grid cells. The rotors aviate 0.12 ADV tilting the rotor disk plane with -1.43 degree. The rotor's operation speed is 37.52 radian per second and the azimuth angle of the rotor blade changes 10 degrees for each time step.

Figure 3 and Figure 4 show the wake structure shed from the coaxial rotor with the rotors and fuselage meshes at the point of top and side view. The wake elements on the wake filaments are convected in the opposite direction of the flight by induced velocities. It can be seen that the strong interaction with shed wake and fuselage lattices occurs at the aft of fuselage plate. This interaction makes unsteadiness and affects the displacements of shed wake elements. After that, some wake elements that penetrating the fuselage surface are eliminated.

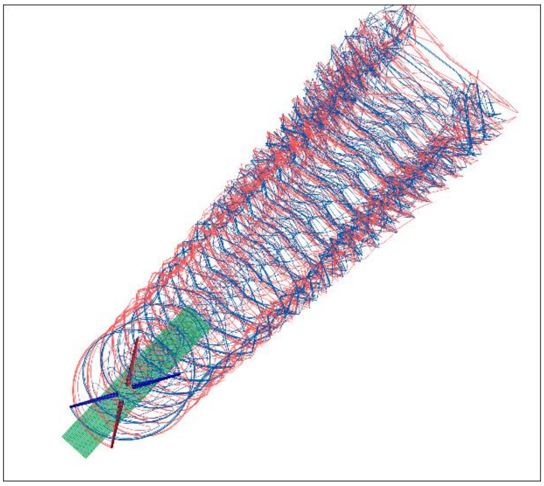

Figure 3 Top view of rotor-fuselage with wake filaments in the flow field

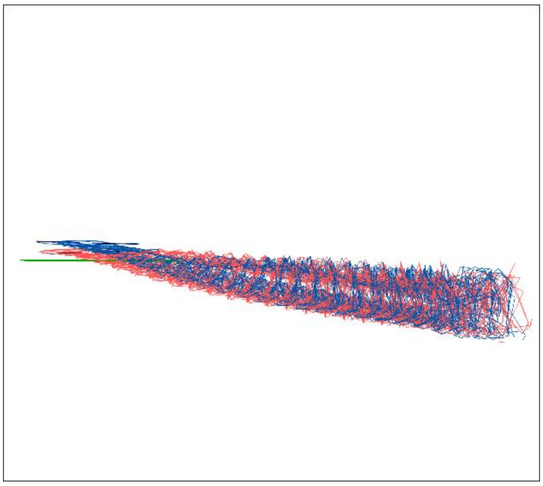

Figure 4 Side view of rotor-fuselage with wake filaments in the flow field

Figure 5 shows the convergence of the average thrust coefficient of coaxial rotor against revolutions. After 4 revolutions, both the isolated coaxial rotor and the coaxial rotor with the fuselage maintain steady thrust coefficient. Though, the isolated one is converged at the 3 revolutions slightly faster than the one with the fuselage at the 4 revolutions. The less thrust fluctuation of the isolated one against revolution can be seen that the one with fuselage influenced by more interactive factors. The isolated one has higher thrust performance than the one with fuselage at the end of the calculation. Figure 6 shows unsteady thrust coefficients of both cases against the azimuth angle within last 2 revolutions. These are described every 10 degrees of the azimuth angle and can analyze more microscopically thrust variations. Due to aerodynamic characteristics of the coaxial rotor, the isolated coaxial rotor also has the fluctuation of the thrust coefficient. The thrust coefficient of the isolated one within 13-15 revolutions are larger than the one with the fuselage, but, the one with fuselage case shows more sharp peaks especially at 5000 degrees of the azimuth angle.

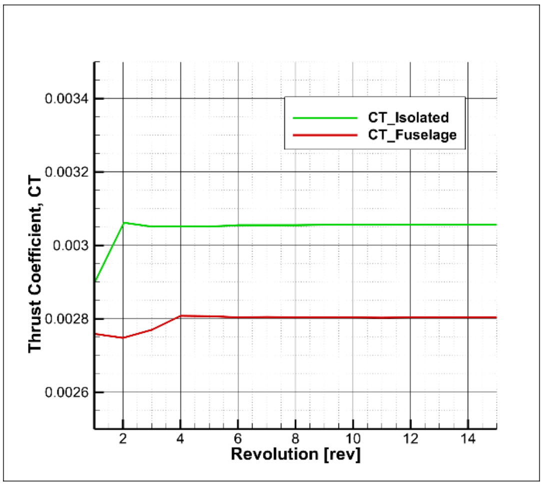

Figure 5 Convergence of thrust coefficient

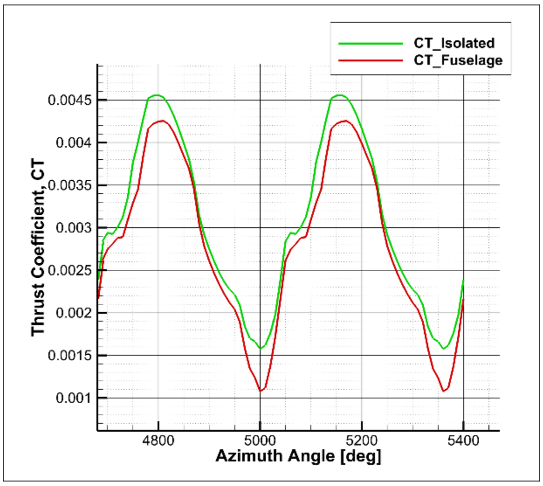

Figure 6 Unsteady thrust coefficient of the blade within 13-15 revolutions

Figure 7 shows the overall sound pressure level against harmonics of BPF (Blade Passing Frequency) compared with the two cases. The observation point of Figure 7 is fore of in-plane (same as the rotor disk plane). In this paper, the OASPL means the sum of discrete frequency noises; the thickness noise and the loading noise. Figure 8 shows OASPL compared with the two cases at out-plane (same as perpendicular to the rotor disk plane). At Figure 7, the OASPL of the coaxial rotor with the fuselage is subtly higher than in almost of BPF regions. Because the loading noise is less dominant than the thickness noise at in-plane and related to the pressure fluctuation, the difference between the two cases is 0.5 dB. It can be seen that the pressure perturbation by the aerodynamic interactions more affects to out-plane overall sound pressure level. In both cases, it can be generally observed that the higher noise levels cover on the rotor disk plane. The maximum distinction within the two configurations is 2.5 dB.

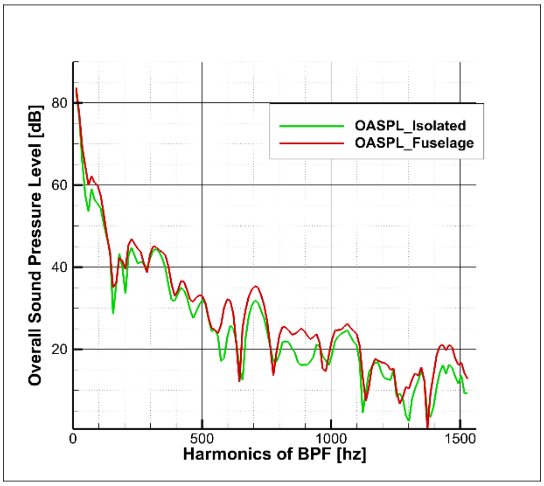

Figure 7 Overall sound pressure level spectrum with multiple of BPF(Blade Passing Frequency)

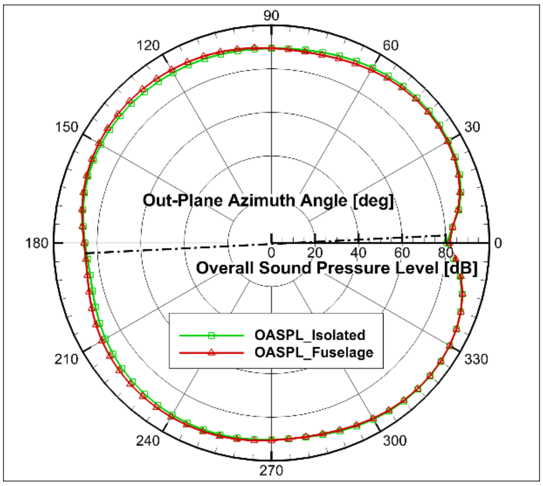

Figure 8 Out-plane overall sound pressure level, Fore(Left), Aft(Right) of rotorcrafts

4. CONCLUSIONS

The numerical simulations have been conducted to study the aerodynamic and aeroacoustics characteristics of the coaxial rotor considering rotor fuselage interaction effect. In this study, simple rectangular source-doublet panel as the fuselage is selected for the analysis, due to the fact that it was a basic research for the coaxial rotor-fuselage interaction phenomena. In order to calculate the complex velocity field generated by the blade, the shed wake, and the fuselage are calculated using free wake vortex lattice method (VLM). FW-H acoustic analogy was used for the impermeable surface to analyze aeroacoustic characteristics considered with the rotor-fuselage interaction effect. The unsteady loadings on the blade were investigated by the unsteady Bernoulli equation. In the case of level flight, the thrust of the coaxial rotor with fuselage case was lower than that of the isolated coaxial rotor configuration at every revolution. Though, the thrust fluctuation affects the unsteady loading noise of the isolated coaxial rotor which is higher than that of the coaxial rotor with fuselage. The noise directivity of the both cases was generally similar in the direction of out-plane, but, the overall sound pressure level of the coaxial rotor with fuselage was subtly bigger at several observation points. Finally, it can be seen that the aeroacoustic characteristics (such as the amplitudes and directivities) of the coaxial rotor with fuselage differ from the isolated coaxial rotor

5. Acknowledgments

This work was conducted at High-Speed Compound Unmanned Rotorcraft (HCUR) research laboratory with the support of Agency for Defense Development (ADD).

6. REFERENCES

1.Colin P. Coleman, "*A Survey of Theoretical and Experimental Coaxial Rotor Aerodynamic Research*", NASA Technical Paper 3675, (1997)
2.Kim, H.W., Duraisamy, K. and Brown, R.E., "*Aeroacoustics of a coaxial rotor in level flight*",64th American Helicopter Society Annual Forum, Montreal, Canada, (2008)
3.M. Mosher and R. L. Peterson, "*Acoustic Measurements of a Full Scale Coaxial Helicopter*", AIAA 8th Aeroacoustics Conference, Atlanta, Georgia, (1983***)***
4.J. C. Wilson and R. E. Mineck, "*Wind-Tunnel Investigation of Helicopter-Rotor Wake Effects on Three Helicopter Fuselage Models*", NASA TM X-3185, (1975)
5. P. F. Sheridan and R. P. Smith, "*International Aerodynamics –A New Challenge to Helicopter Technology*", Journal of the American Helicopter Society, (1980)
6.J. Jang and S. Park, "*Prediction of Fuselage Surface Pressure in Rotor-Fuselage Interactions Using an Integral Formulation of Poisson Equation*", Asian/Australian Rotorcraft Forum, (2013)
7.J. Katz and A. Plotkin, "*Low-Speed Aerodynamics*," 2nd ed., Cambridge University Press, (2001)
8. D. B. Bliss, M. E. Teske and T. R. Quackenbush, "*A New Methodology for Free Wake Analysis Using Curved Vortex Elements*", NASA CR 3958, (1987)
9.M. P. Scully, "*Computation of Helicopter Rotor Wake Geometry and its Influence on Rotor Harmonic Airloads*", ASRL TR 178-1, (1975)
10. Gennaretti, M., and Bernardini, G., "*Novel Boundary Integral Formulation for Blade-Vortex Interaction Aerodynamics of Helicopter Rotors*," *AIAA Journal* (2007)

11.J. E. Ffowcs Williams and D. L. Hawkings, "*Sound Generation by Turbulence and Surfaces in Arbitrary Motion*", Philosophical Transactions for the Royal Society of London. Series A, Mathematical and Physical Sciences, (1969)
12. Mineck, R. E., and Gorton, A. S., "*Steady and Periodic Pressure Measurements on a Generic Helicopter Fuselage Model in the Presence of a Rotor*", NASA TM 2000-210286, (2000)